Chapter 5

Electromagnetic Wellbore Heating

Ibrahim Agyemang[1], Matthew Bolton[2], Lloyd Bridge[2], Samantha Carruthers[3], Tom Janiewicz[4], Margaret Liang[2], Leevan Ling[4], Bruce McGee[5], Andrea McPhee[6], Dominique Noel[1], David Ross[7], Maurice Shevalier[8], Sirod Sirisup[9], Daniel Spirn[10], Ranga Sreenivasan[8], Jef Williams[4].

Report prepared by C. Sean Bohun[3].

5.1 Introduction

This paper is concerned with the recovery of petroleum fluids from an oil reservoir using electrical energy. By its very nature this problem must deal with both the equations that describe the fluid flow as well as the heat flow equations. In general, the oil in the wellbore is very viscous with the consequence that the fluid moves slowly. As a result, the amount of oil collected in a given time is quite small. To increase the production rate of the well, the oil's velocity needs to be increased. One method of accomplishing this is by heating the fluid using an electromagnetic induction tool (EMIT). The simple principle behind the EMIT is that it heats the fluid thereby decreasing its viscosity and increasing its velocity. This method of increasing the production rate of a given wellbore is currently being utilized with the generalization that for wells of several hundred metres in length, several EMIT regions are placed in the wellbore at intervals of about one hundred metres. So that they are all supplied sufficient power, these EMIT regions are connected by a cable surrounded by a steel housing.

We are interested in developing a mathematical model of this problem with the ultimate

[1]University of Alberta
[2]University of British Columbia
[3]University of Victoria
[4]Simon Fraser University
[5]McMillan-McGee Corporation
[6]University of Toronto
[7]Eastman Kodak
[8]University of Calgary
[9]McGill University
[10]New York University

goal of investigating analytically the relationship between the temperature of the EMIT and the production rate of the oil.

One approach to this problem is to write out the full system of coupled partial differential equations that relate the temperature and the velocity flux and then to solve them numerically with an expensive computational fluid dynamics (CFD) program. Indeed, this method has been used in the past [4] and it will be used to test the accuracy of our simplified model in the absence of experimental data. The purpose of *this* paper is to carefully analyse each of the physical processes in this system and by making some basic assumptions, to derive a simple set of equations that still captures the main features of the system modelled with the CFD code.

This paper is organised in the following way. Section 5.2 describes the overall geometry of the problem and establishes the coordinates used to describe the model. At this point the problem is broken into three subproblems: i) the flow of fluid in the reservoir, ii) the flow of fluid in the wellbore and iii) the generation of temperature from the heat sources in any EMIT regions. Parts i) and ii) result in a second order ODE for the oil flux for a fixed viscosity. From part iii) it is found that the temperature of the fluid is inversely proportional to the velocity. Fluid that moves slowly past an EMIT region will absorb more heat than the same amount of fluid that moves quickly past an EMIT. As a result, slowing the fluid velocity increases the temperature and therefore decreases the viscosity. This viscosity is used in parts i) and ii) thereby closing the system of equations.

Part i) is described in section 5.3, where a relationship between the axial changes in the fluid flux and the pressure in the wellbore is derived. The details of part ii) can be found in section 5.4 where a relationship for the velocity and the pressure from the Navier-Stokes equations is obtained by averaging over the radius of the wellbore. Under the assumptions made, the pressure is found to be related to the radius of the wellbore by a form of Poiseuille's law.

Finally, section 5.5 details the derivation of part iii), the temperature equations. This derivation is complicated by the fact that there are four radial regions of the radial problem to consider; EMIT, casing, reservoir and wellbore with the first three forming the boundary conditions for the heat equation in the wellbore region. Furthermore, there are three axial regions: EMIT region, cable region, and a region where there is neither EMIT nor cable. Section 5.6 pulls the results of sections 5.3, 5.4 and 5.5 together and section 5.7 illustrates the analytical solution of the resulting model in the simple situation when no heat is applied to the oil.

In section 5.8, we discuss numerical results of the simplified model with respect to the results predicted by the CFD code. On comparison, we find considerable qualitative agreement between the two models which is quite remarkable considering their relative complexities. These aspects are further discussed in the final section of the paper.

5.2 Geometry

Figure 5.1 depicts the overall geometry of the problem. A horizontal cylindrical well extends from $z = 0$ to $z = L$. Fluid flows radially into the well from the surrounding media and is drawn out with a pump which is located at $z = L$ where a fixed pressure of P_P is maintained.

At $z = 0$, where the end cap is situated, the motion of the flow is radially inward (no horizontal flow at this point). As one increases in z, the action of the pump comes into effect

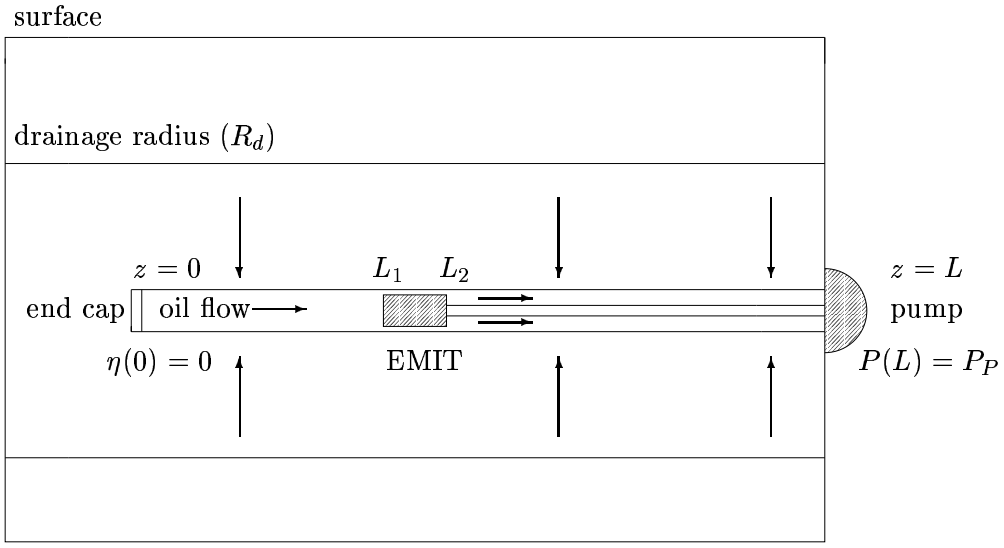

Figure 5.1: Overall geometry for the horizontal wellbore problem.

and imparts a horizontal component to the fluid flow.

This figure shows only one EMIT region which extends from $z = L_1$ to $z = L_2$. It is in these EMIT regions that the oil is heated. Power is supplied to the EMITs through a cable housing resulting in three different regions. Starting at the pump we have a cable housing region that extends to the first EMIT. If there are other EMIT regions then they must also be joined with cable housing and eventually, after the last EMIT region, the wellbore is open with no impediment to the horizontal flow.

5.3 Axial Velocity: Darcy's Law

Once the horizontal well is drilled, fluid seeps from the surrounding region into the wellbore. Once inside the wellbore, the fluid is drawn out with a pump that maintains a fixed pressure at one end of the well. The rate at which the fluid seeps into the wellbore is a function of the pressure differential and the viscosity of the fluid. Indeed, the flow rate (volume/time) of the fluid into a segment of the wellbore of length Δz is given by the expression [2]

$$q(z) = \frac{2\pi k[P_R - P(z)]}{\mu_o \ln(R_d/R_c)}\Delta z \tag{5.1}$$

where k is the permeability of the reservoir, P_R is the reservoir pressure, $P(z)$ is the pressure inside the wellbore at the axial position z, μ_o is the viscosity at the ambient temperature T_a, R_d is the drainage radius and R_c is the outer radius of the casing.

Since we are assuming that we are at a steady state, we make the assumption that the radially flowing fluid remains unheated until it reaches the inner radius of the casing at which point it instantly becomes heated to the temperature of the fluid at that particular z position. Consequently the viscosity in expression (5.1) will remain as μ_o even once the temperature of the wellbore is increased.

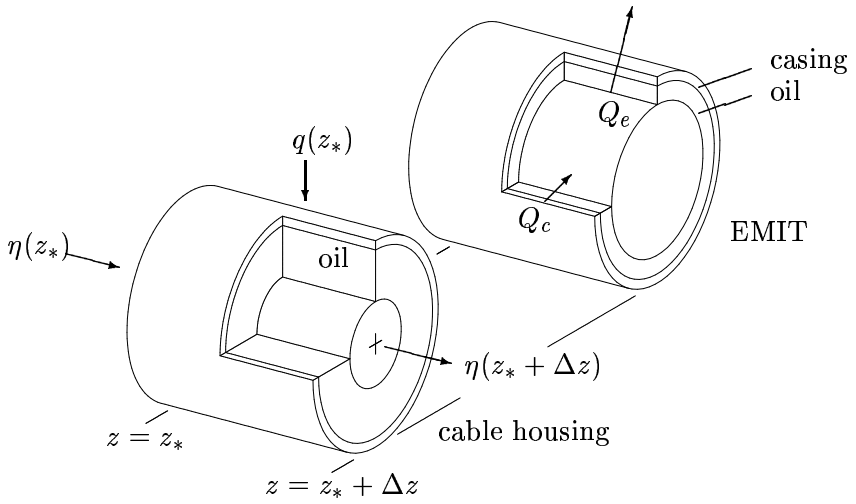

Figure 5.2: An infinitesimal section of the wellbore for the EMIT or cable housing regions.

Using equation (5.1) one can find an expression for the average axial velocity of the fluid, $\bar{v}(z)$. Let R_z denote the inner radius of the wellbore which could be zero, the radius of the EMIT tool, R_e, or the outer radius of the electrical housing, R_h. Using this definition of R_z, let $\eta(z) = \pi(R_w^2 - R_z^2)\bar{v}(z)$ which is the flux in the wellbore. The advantage of using $\eta(z)$ rather than $\bar{v}(z)$ is that $\eta(z)$ is a continuous function whereas the velocity $\bar{v}(z)$ is not.

Figure 5.2 shows an infinitesimal annular section of the wellbore of length Δz. At $z = z_*$ the axial flux is $\eta(z_*)$ while the radial flux is given by expression (5.1). By the conservation of mass, these two components combine to give the axial flux at $z = z_* + \Delta z$. In other words,

$$\eta(z_*) + \frac{2\pi k[P_R - P(z_*)]}{\mu_o \ln(R_d/R_c)}\Delta z = \eta(z_* + \Delta z).$$

Rearranging terms and letting $\Delta z \to 0$ gives the expression

$$\frac{d\eta}{dz} = \frac{2\pi k[P_R - P(z)]}{\mu_o \ln(R_d/R_c)}; \qquad \eta(0) = 0. \tag{5.2}$$

The boundary condition $\eta(0) = 0$ just expresses our approximation that the axial fluid velocity is zero at the end of the wellbore. Since $P(z) < P_R$ throughout the wellbore, $d\eta/dz > 0$ which is consistent with having the fluid flux increase as it approaches the pump located at $z = L$.

5.4 Axial Pressure: Navier-Stokes

A relationship between wellbore pressure and flow velocity is obtained from the Navier-Stokes equations for an incompressible[11] viscous fluid,

$$\rho\frac{\partial \vec{v}}{\partial t} + \rho(\vec{v}\cdot\nabla)\vec{v} = -\nabla P + \mu\Delta\vec{v}. \tag{5.3}$$

[11] A fluid is said to be incompressible if the velocity satisfies $\nabla \cdot \vec{v} = 0$.

Again refer to figure 5.2 where we consider an arbitrary yet constant cross section. Assume a steady fluid flow inside the wellbore that propagates in the $\hat{\mathbf{k}}$ direction. Assuming that the flow is radially symmetric, we have $\vec{v} = v(r)\hat{\mathbf{k}}$ and the continuity equation is automatically satisfied. Resolving (5.3) into the r, θ and z directions gives $\partial P/\partial r = 0 = \partial P/\partial\theta$ and

$$\mu \frac{1}{r}\frac{\partial}{\partial r}\left(r\frac{\partial v}{\partial r}\right) = \frac{\partial P}{\partial z}. \tag{5.4}$$

The first two conditions on the pressure imply that $P = P(z)$. As a consequence, the RHS of (5.4) is a function of z alone while the LHS is a function of r alone. The only way that this can be so is if the pressure is constant over the cross-section of the wellbore. This implies that for our annular domain $R_z < r < R_w$ and $z_* < z < z_* + \Delta z$ we must solve

$$\mu \frac{1}{r}\frac{\partial}{\partial r}\left(r\frac{\partial v}{\partial r}\right) = \frac{\Delta P}{\Delta z}; \qquad v(R_z) = 0 = v(R_w)$$

where $\Delta P = P(z_* + \Delta z) - P(z_*) < 0$ and we have imposed a no slip condition on the boundary. The general solution for the velocity distribution as a function of radius in this case is found to be

$$v(r) = \frac{1}{4\mu}\frac{\Delta P}{\Delta z}\left[r^2 - R_w^2 - \frac{R_w^2 - R_z^2}{\ln(R_w/R_z)}\ln\left(\frac{r}{R_w}\right)\right].$$

For regions in which there is no EMIT tool or tubing ($R_z = 0$), this reduces to the familiar parabolic flow profile

$$v(r) = \frac{1}{4\mu}\frac{\Delta P}{\Delta z}(r^2 - R_w^2).$$

In order to find the average flux of oil at any fixed value of z one needs to compute the average of this radial velocity. Computing this average results in

$$\overline{v} = \frac{2}{(R_w^2 - R_z^2)}\int_{R_z}^{R_w} v(r)\, r dr = \frac{1}{8\mu}\frac{\Delta P}{\Delta z}\left[\frac{R_w^2 - R_z^2}{\ln(R_w/R_z)} - \frac{R_w^4 - R_z^4}{R_w^2 - R_z^2}\right].$$

If we now let $\Delta z \to 0$, rearrange terms and use the definition of η this becomes

$$\frac{dP}{dz} = -\frac{8\mu}{\pi}\left[\frac{\ln(R_w/R_z)}{(R_w^4 - R_z^4)\ln(R_w/R_z) - (R_w^2 - R_z^2)^2}\right]\eta(z); \qquad P(0) = P_P \tag{5.5}$$

where P_P is the pressure maintained by the pump at $z = L$. If one allows $R_z \to 0^+$ then equation (5.5) reduces to

$$\frac{dP}{dz} = -\frac{8\mu}{\pi R_w^4}\eta(z)$$

which is the popular *Hagen-Poiseuille* [1] equation. We have now reached the point where we can consider what happens as the wellbore is heated.

Data	Symbol	Value
Wellbore Properties		
Outer Casing Radius	R_c	69.85 mm
Inner Casing Radius	R_w	63.50 mm
EMIT Radius	R_e	50.80 mm
Housing Radius	R_h	30.1625 mm
Left Edge of EMIT	L_0	495 m
Right Edge of EMIT	L_1	505 m
Wellbore Length	L	1,000 m
Reservoir Properties		
Permeability[12]	k	10,000 mD
Ambient Viscosity[13]	μ_o	15,000 cP
Drainage Radius	R_d	100 m
Reservoir Pressure[14]	P_R	5,000 kPa
Producing Pressure	P_P	500 kPa
Thermal Properties		
Fluid Heat Capacity	ρC_f	2.8×10^6 J m^{-3}K^{-1}
Casing Power	Q_c	795.8 kW m^{-3}
EMIT Power	Q_e	79.58 kW m^{-3}
Ambient Temperature	T_a	30°C

Table 5.1: Input Data for the example calculations.

5.5 Including the Temperature

For the purposes of this discussion, we assume that the wellbore has a steady state temperature distribution that is a function of r and z alone. As well, to simplify the expressions, we will take the far field temperature to be zero. We also assume that thermal conduction in the z direction is negligible. The primary sources of heat are the EMIT regions and the casings around them and it is assumed that the heat production is uniform. Since the reservoir and casings are porous,[15] heat is convected radially in them. In the wellbore, oil flows along the axis and therefore heat is convected axially in the wellbore.

Consider the casing. In this region, the total rate of heat flow is the sum of the flow due to heat conduction and the flow due to the movement of fluid in the radial direction. The result of this is that the heat flux in the casing is given by

$$\vec{\Phi}_c = \left(\lambda_c \frac{\partial u}{\partial r} + \rho C_f v_r u \right) \hat{\mathbf{r}}. \tag{5.6}$$

We have denoted the temperature as $u(r, z)$, the radial speed of the fluid as v_r, the conductivity

[12] 1 darcy = 9.86923×10^{-13} m^2.
[13] 1 centipoise = 1×10^{-3} kg m^{-1}s^{-1}.
[14] 1 pascal = 1 kg m^{-1}s^{-2}.
[15] The casing actually has holes drilled into it for the transport of oil.

of the casing as λ_c and ρC_f for the fluid heat capacity.

For any closed region the total heat energy produced must equal the total heat energy lost. Let Q_c be the amount of heat energy produced in the casing per volume per unit time. By choosing a cylindrical region of radius r and length Δz expression (5.6) implies that

$$2\pi\Delta z\left(\lambda_c r\frac{\partial u}{\partial r}+\rho C_f r v_r u\right)+2\pi\Delta z\int Q_c\, r dr=0 \qquad \text{or} \qquad \frac{1}{r}\frac{\partial}{\partial r}\left(\lambda_c r\frac{\partial u}{\partial r}+\beta u\right)+Q_c=0 \tag{5.7}$$

where $\beta=\rho C_f r v_r$. A similar line of reasoning yields expressions for the reservoir, wellbore and EMIT. These equations are summarized below:

$$\text{Reservoir:} \qquad \frac{1}{r}\frac{\partial}{\partial r}\left(\lambda_r r\frac{\partial u}{\partial r}+\beta u\right)=0 \tag{5.8}$$

$$\text{Wellbore:} \qquad \frac{1}{r}\frac{\partial}{\partial r}\left(\lambda_w r\frac{\partial u}{\partial r}\right)=\frac{\rho C_f}{\pi}\frac{\partial}{\partial z}(\eta u) \tag{5.9}$$

$$\text{EMIT:} \qquad \frac{1}{r}\frac{\partial}{\partial r}\left(\lambda_e r\frac{\partial u}{\partial r}\right)+Q_e=0. \tag{5.10}$$

We are not interested in resolving the details of the radial temperature distribution in the wellbore. Rather, we only care about the axial variations of the mean temperature. This permits a simplification. First define the mean temperature over the wellbore cross-section at z to be

$$T(z)=\frac{2}{(R_w^2-R_z^2)}\int_{R_z}^{R_w}u(r,z)\,r dr$$

as we did with η in the derivation of equation (5.5). Recall that R_z is the inner radius and depends on z. With this definition, the equation for the wellbore (5.9) can be integrated resulting in the expression

$$\rho C_f(R_w^2-R_z^2)\frac{d}{dz}(\eta T)=2\pi\lambda_w r\frac{\partial u}{\partial r}\Big|_{R_z}^{R_w}. \tag{5.11}$$

The thermal flux in the wellbore is given by

$$\vec{\Phi}_w=\lambda_w\frac{\partial u}{\partial r}\hat{\mathbf{r}}+\frac{\rho C_f\eta u}{\pi r^2}\hat{\mathbf{k}}.$$

This must be continuous at the interfaces. Hence in the radial direction for the wellbore/casing and wellbore/EMIT interfaces one has respectively

$$r\lambda_w\frac{\partial u}{\partial r}\Big|_{R_w}=\left(r\lambda_c\frac{\partial u}{\partial r}+\beta u\right)\Big|_{R_w} \qquad \text{and} \qquad r\lambda_w\frac{\partial u}{\partial r}\Big|_{R_z}=r\lambda_e\frac{\partial u}{\partial r}\Big|_{R_z}.$$

It remains for us to evaluate these fluxes.

By solving (5.10) we find that

$$\lambda_e r\frac{\partial u}{\partial r}\Big|_{R_z}=-\frac{1}{2}Q_e R_z^2. \tag{5.12}$$

Furthermore, by solving (5.8) one finds that the temperature has the general form

$$u(r,z) = k_1 + k_2 r^{-\beta/\lambda_r}$$

where k_1 and k_2 are constants. Because the far field temperature is zero, one must have $T(\pm\infty, z) = k_1 = 0$. As a result,

$$\lambda_r r \frac{\partial u}{\partial r} + \beta u = \beta k_1 = 0. \tag{5.13}$$

So the thermal flux in the reservoir and, in particular, the thermal flux through the casing/reservoir interface is zero. Using this as a boundary condition one can integrate the expression for the casing (5.7) to find that

$$\left(\lambda_c r \frac{\partial u}{\partial r} + \beta u\right)\Big|_{R_w} = \frac{1}{2} Q_c (R_c^2 - R_w^2). \tag{5.14}$$

Collecting equations (5.11)-(5.14) gives the final result that

$$\rho C_f \frac{d}{dz}[\eta(z)\, T(z)] = \pi \left[Q_c(z)(R_c^2 - R_w^2) + Q_e(z) R_e^2\right]; \qquad T(0) = 0. \tag{5.15}$$

The heat sources Q_c and Q_e have been written as functions of z. If one is not in an EMIT region, these functions are simply zero. As a result, the RHS of (5.15) piecewise constant; nonzero only where an EMIT is located. Integrating (5.15) gives the result that

$$T(z) = \begin{cases} 0; & 0 \le z < L_0 \\ \dfrac{\Omega}{\eta(z)} \dfrac{z - L_0}{L_1 - L_0}; & L_0 \le z < L_1 \\ \dfrac{\Omega}{\eta(z)}; & L_1 \le z \le L, \end{cases} \qquad \Omega = \frac{\pi[Q_c(R_c^2 - R_w^2) + Q_e R_e^2](L_1 - L_0)}{\rho C_f}. \tag{5.16}$$

From the values in table 5.1 we find that $\Omega \sim 3.10 \times 10^{-2}$ $\mathrm{m^3 s^{-1} K}$. Notice that if $\eta(z)$ were constant then the temperature would increase monotonically as one moved from $z = 0$ to $z = L$. However, since $\eta(z)$ actually increases as one moves toward the pump, the temperature of the fluid must decrease once it passes an EMIT region.

The temperature affects the velocity and the pressure through the viscosity. This viscosity is given empirically in units of thousands of centipoise through

$$\log_{10} \mu(T) = -3.002 + \left(\frac{453.29}{303.5 + T}\right)^{3.5644}. \tag{5.17}$$

Hence, one can see that an increase of 100°C can result in a decrease in viscosity of about three orders of magnitude. One final point is that the far field temperature should correspond to the ambient viscosity μ_0. Since $\mu_0 = 15000$ cP we associate the far field temperature of zero with the ambient temperature of $T_a = 30$°C.

5.6 Velocity, Pressure, Temperature Summary

In the axial direction, the rate of change of $\eta(z) = \pi(R_w^2 - R_z^2)\bar{v}(z)$ is governed by Darcy's Law and in our approximation it is assumed that the fluid is not heated until it reaches the wellbore. For the axial pressure, the Navier-Stokes equations are solved for an annular region by assuming that the fluid is incompressible. When we apply heat to wellbore, it is this fluid in the wellbore that is heated and not the fluid in the surrounding region. Therefore by combining the equations (5.2) and (5.5) we can summarize the problem for $\eta(z)$ as

$$\frac{d^2\eta}{dz^2} - \frac{16k\Gamma(z)}{\ln(R_d/R_c)}\frac{\mu(T(z))}{\mu_o}\eta = 0; \qquad \eta(0) = 0, \quad \frac{d\eta}{dz}\Big|_L = \frac{2\pi k(P_R - P_P)}{\mu_o \ln(R_d/R_c)},$$
$$\Gamma(z) = \frac{\ln(R_w/R_z)}{(R_w^4 - R_z^4)\ln(R_w/R_z) - (R_w^2 - R_z^2)^2}$$

where the temperature as a function of z is given with the expression (5.16) and the viscosity μ is given explicitly by (5.17). Recall that $\mu_o = \mu(0)$. So we see that under the assumptions, this problem reduces to finding the solution of a second order nonlinear *ordinary* differential equation for $\eta(z)$.

Once we have solved for $\eta(z)$, relation (5.16) determines the temperature profile and consequently the viscosity as a function of z. The pressure as a function of z is given by expression (5.2) with the result that

$$P(z) = P_R - \frac{\mu_o}{2\pi k}\ln\left(\frac{R_d}{R_c}\right)\frac{d\eta}{dz}. \tag{5.18}$$

Notice that since η increases monotonically as one approaches the pump, the slope of η is positive definite. Consequently, the pressure decreases monotonically as one approaches the pump. One can also extract the average velocity and the production rate at the pump from η. The velocity is given by $\bar{v}(z) = \eta(z)/(\pi(R_w^2 - R_z^2))$ and the volume flux at the pump is $\eta(L)$.

5.7 An Illustrative Example

The overall characteristics of our model can be extracted by studying the case when there are no EMIT regions. In this case one has $Q_c(z) \equiv 0$ and $Q_e(z) \equiv 0$ and from equations (5.16) and (5.17), $\mu(T(z)) = \mu(0) = \mu_o$. In addition, $R_z = 0$ so that $\Gamma(z) = 1/R_w^4$ and the equation for $\eta(z)$ reduces to

$$\frac{d^2\eta}{dz^2} - \frac{16k}{R_w^4\ln(R_d/R_c)}\eta = 0; \qquad \eta(0) = 0, \quad \frac{d\eta}{dz}\Big|_L = \frac{2\pi k(P_R - P_P)}{\mu_o \ln(R_d/R_c)}.$$

The explicit form of the solution is easily verified to be

$$\eta(z) = \frac{\pi R_w^4}{8\mu_o}\frac{P_R - P_P}{L_{\text{crit}}}\frac{\sinh\gamma z}{\cosh\gamma L}; \qquad L_{\text{crit}}^2 = \frac{R_w^4}{16k}\ln\left(\frac{R_d}{R_c}\right) = \frac{1}{\gamma^2}.$$

From expression (5.18) the corresponding pressure is

$$P(z) = P_R - (P_R - P_P)\frac{\cosh\gamma z}{\cosh\gamma L}.$$

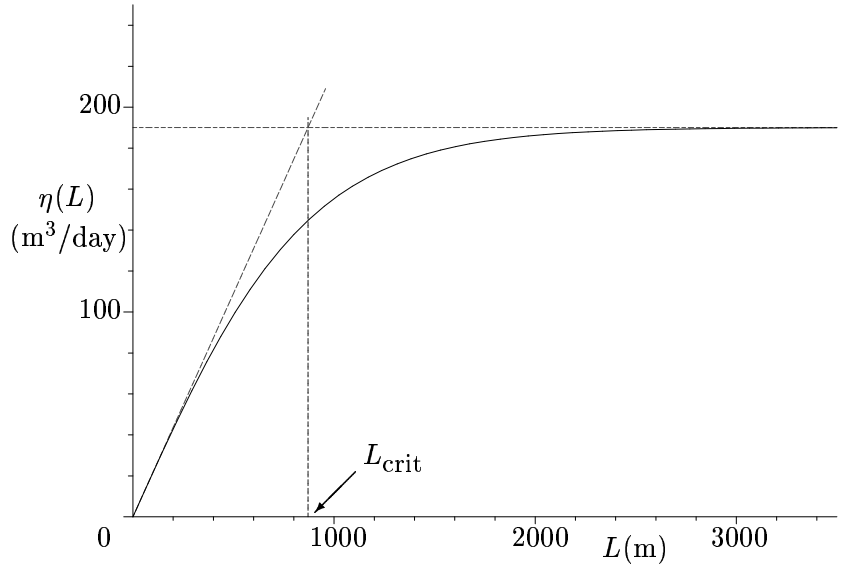

Figure 5.3: The production rate at the pump as a function of the length of the wellbore.

The total production rate at the pump is given by the revealing expression

$$\eta(L) = \frac{\pi R_w^4}{8\mu_o}\frac{P_R - P_P}{L_{\mathrm{crit}}}\tanh\gamma L \sim \begin{cases} \dfrac{\pi R_w^4}{8\mu_o}\dfrac{P_R - P_P}{L_{\mathrm{crit}}}; & L \gg L_{\mathrm{crit}} \\ \dfrac{\pi R_w^4}{8\mu_o}\dfrac{P_R - P_P}{L_{\mathrm{crit}}}\dfrac{L}{L_{\mathrm{crit}}}; & L \ll L_{\mathrm{crit}} \end{cases}$$

which is depicted in figure 5.3 for the data given in table 5.1 where $L_{\mathrm{crit}} = 865$ m and the maximum production rate is 191.32 $\mathrm{m}^3\mathrm{day}^{-1}$. What is immediately apparent is that, without heating, drilling a horizontal well beyond the critical length will not yield any significant increase in production.

5.8 Results

As we stated in the introduction, the agreement between the qualitative results of the simplified model and those predicted by the CFD code are quite remarkable. This is especially true in light of their respective computational costs. Figure 5.4 illustrates the results for the data described in table 5.1.

Only the pressure, temperature and final production rate are easily available from the CFD code. Because of this, only the pressure and temperature curves in figure 5.4 have a dashed line. To solve the nonlinear ODE described in section 5.6 two different method were employed; a shooting method and a method of successive over relaxation (SOR). Whenever they are discernible, the solution from the shooting method is a solid line while the SOR solution is a dashed dot line. We begin our discussion with the pressure curve.

Because of the boundary condition $P(L) = P_P$, all of the pressure curves intersect at $z = L$. At $z = 0$ the CFD code predicts that $P_{\mathrm{cfd}}(0) = 4.07 \times 10^3$ kPa while the solution of the simplified model gives $P_{\mathrm{sm}}(0) = 3.44 \times 10^3$ kPa. Despite the fact that our model tends to

underestimate the results from the CFD code, the amount of pressure drop across the EMIT region is predicted correctly. $P_{\text{sm}}(z)$ can be made to match $P_{\text{cfd}}(z)$ by artificially decreasing the outer casing radius R_c however this would in turn decrease the predicted production rate. These observations indicate that the differences in the pressure predicted with the simplified model and the CFD code are greatest where the fluids tend to form a boundary layer on the outer casing wall. The last curve in this plot is solely for comparison purposes. It is the pressure curve for the example described in section 5.7 where there is no EMIT region.

Comparing the temperature curves, there is a distinct difference in the shape of the two curves. However, the temperature from the CFD code is just the temperature at a fixed radius rather than an average over the radius of the wellbore for a given value of z. The peak temperature in the EMIT region is faithfully reproduced, but the rate at which the fluids lose heat is larger in the CFD model. Consequently, the surface temperature of simplified model is larger, $T_{\text{sm}}(L) = 37.4^o\text{C}$, than that of the CFD model, $T_{\text{cfd}}(L) = 33.1^o\text{C}$. Curves for the viscosity and the velocity could not be compared with the CFD model as these quantities were not directly accessible.

For the production rate refer to figure 5.5. As can be seen, the simplified model underestimates the production rate at the pump. In fact, $\eta_{\text{cfd}}(L) = 187.6$ m^{3}day^{-1} while $\eta_{\text{sm}}(L) = 115.2$ m^{3}day^{-1}. This can also be explained with the formation of a boundary layer. In the full model the boundary layer for the cool fluids to the left of the EMIT region would extend further into the wellbore than in the region to the right of the EMIT where the fluid is heated. This relative difference in the effective outside radius of the casing due to a boundary layer of varying thickness would tend to boost the overall production rate.

In general, the simplified model seems to reproduce the overall characteristics of the full model described by the CFD code. Moreover, it does this with a comparatively low computational cost. One of the primary benefits of this reduction in the computational cost is that it allows one to run a number of numerical experiments cheaply and *on site* in the vicinity of the wellbore itself. As an example, for a given set of wellbore characteristics, we can quickly iterate the simplified model to search for the position of the EMIT which maximizes the production rate at the pump. Because of the inherent nonlinearity, it is not at all clear that this position should simply be the midpoint $z = L/2$. While there will be a unique location that yields a global maximum for the production rate, it is not at all clear that there can not be other local maxima or minima. From figure 5.5 we know that for the geometry in table 5.1 that $\eta_{\text{sm}}(L) = 115.2$ m^{3}day^{-1} when the EMIT is located at $L/2$. The complete curve where the EMIT is allowed to move from one end of the wellbore to the other is shown in figure 5.6. One finds that the greater the distance between the EMIT and the pump, the greater the production. However at about $z = 0.40L$ the rate of increase in production begins to flatten out. Moving the EMIT tool 100 m for an increase of only 1% in production rate at the pump hardly seems worth the effort. Placing the centre of the EMIT at 400 m yields a production rate of at the pump of $\eta_{\text{sm}}(L) = 116.6$ m^{3}day^{-1}. From our observations of the two models, the production rate predicted by the CFD code will of course be greater than this, but more importantly, it should be greater than $\eta_{\text{cfd}}(L) = 187.6$ m^{3}day^{-1} obtained when the EMIT region is located at $L/2$.

5.9 Conclusions and Recommendations

We present a mathematical model for the flow of fluids in a horizontal well in which the well has one or more regions that are electrically heated from an external source. By making some basic assumptions, we develop a nonlinear second order *ordinary* differential equation for the volume flux $eta(z)$ as a function of distance along the wellbore. From the volume flux, both the average radial temperature and the pressure can be extracted. This model succeeds in capturing many of the features observed in the solutions presented with an expensive computational fluid dynamics (CFD) program. Our model tends to underestimate both the pressure and the production rate however, it retains the overall structure of these quantities. The large reduction in computational cost when using the simplified model allows one to quickly run a series of numerical experiments to see the effects of changing various parameters. One such experiment is considered and it is found if the wellbore extends from $z = 0$ to $z = L$ with the pump at $z = L$ then the EMIT should be placed at about $z = 0.40L$ to maximize the production. While the production rate could be increased further by moving the EMIT closer to $z = 0$, this would only increase the production rate a mere 1-2%.

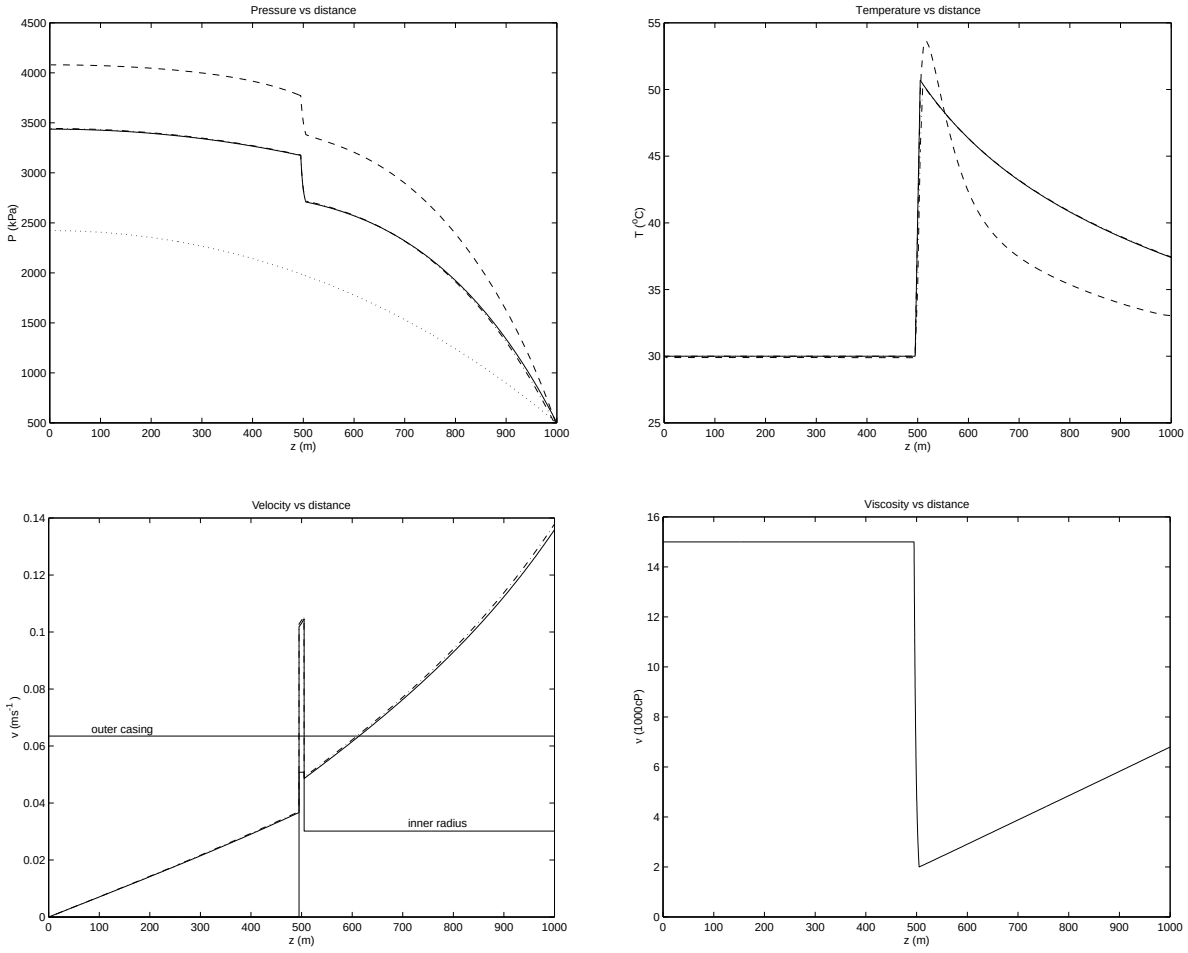

Figure 5.4: The four figures are the pressure, temperature, velocity and viscosity as a function of distance along the wellbore. Only the pressure and temperature for the CFD code was available. These are the dashed lines in the respective plots. More than one method was used to solve the simplified model. Where they are distinguishable, the shooting method solution is a solid line where the SOR method is indicated with a dashed dot. A longitudinal section of the wellbore in indicated in the plot of the velocity.

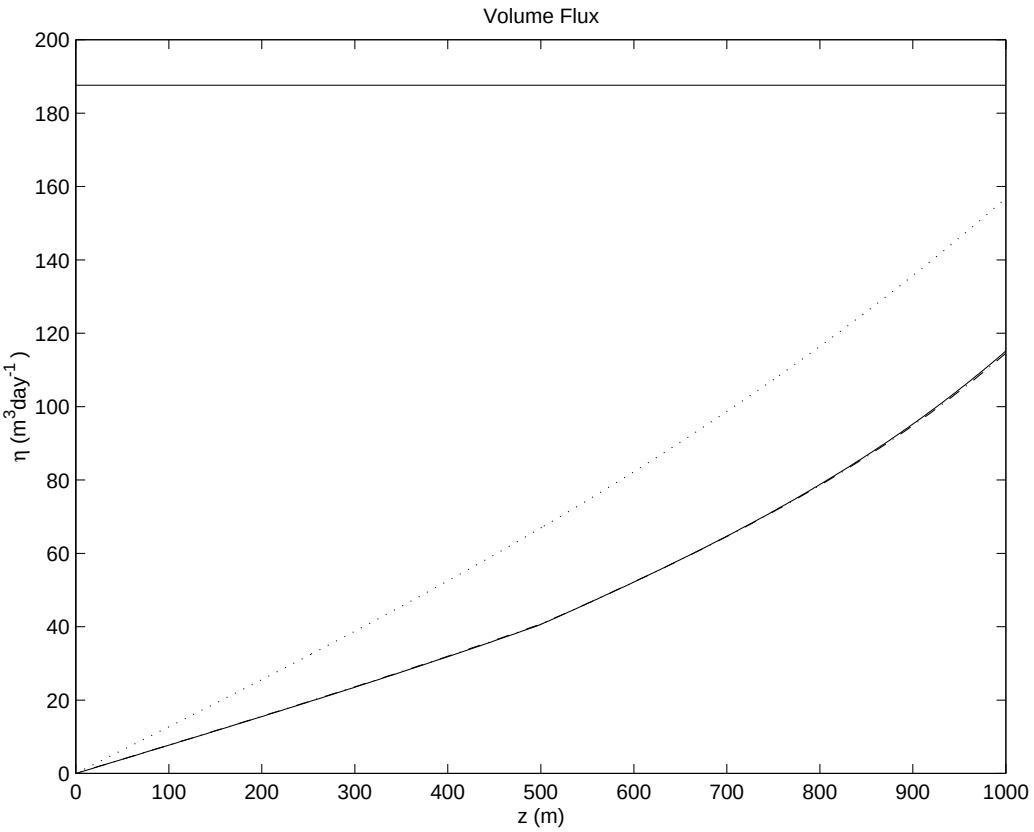

Figure 5.5: The production rate $\eta_{\mathrm{sm}}(z)$ as a function of distance along the wellbore for the simplified model. Only the production at the pump $\eta_{\mathrm{cfd}}(L)$ was available from the CFD code. The dotted curve is the production rate for the case of no EMIT described in section 5.7.

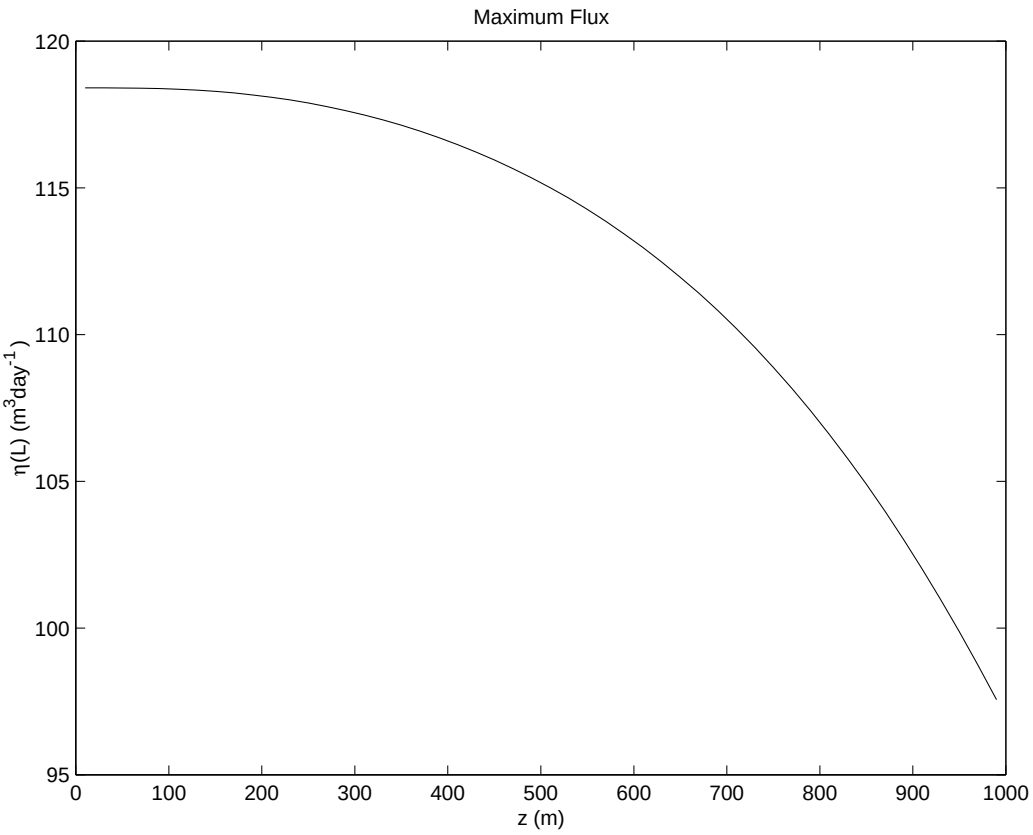

Figure 5.6: The production rate at the pump $\eta_{\mathrm{sm}}(L)$ as a function of the location of the centre of the EMIT.

Bibliography

[1] Landau, L.D. & Lifshitz, E.M., (1959). *Fluid Mechanics.* Addison-Wesley Series in Advanced Physics. Pergamon Press Ltd.: Reading Massachusetts. pp. 56-57.

[2] Hubbert, K.M., (1956). *Darcy's Law and the Field Equations of the Flow of Underground Fluids.* Petroleum Transactions, AIME, Vol. 207, pp. 222-239.

[3] Myint-U, T., (1973). *Partial Differential Equations in Mathematical Physics.* American Elsevier Publishing Company Inc.: New York.

[4] Vinsome, P.K.W., McGee, B.C.W., Vermeulen, F.E. & Chute, F.S, (1994). *Electrical Heating.* Journal of Canadian Petroleum Technology, Vol. 33, No. 9, pp. 29-35.